

# Flux-Coupled Direct Feedback in a SQUID Amplifier

Bruce A. Hines, Kyle M. Sundqvist, Dennis N. Seitz, Martin E. Huber

**Abstract**—The Cryogenic Dark Matter Search (CDMS) employs dc superconducting quantum interference device (SQUID) series array amplifiers (SSAAs) in its phonon readout system. These amplifiers are in a transresistance topology utilizing feedback from room-temperature electronics. The input coil of each SSAA is in series with a phonon sensor composed of many parallel transition edge sensors (TES's). The SSAA consists of 100 individual SQUIDs, each surrounded by planar input and feedback coils with an electrically isolated flux-focusing washer, which increases the inductive coupling between the SQUID and each coil. A room-temperature gain stage completes the feedback loop between the SSAA output voltage and the feedback coil current. We report on a significant mutual inductance that exists directly between the feedback and input coils, on its impact on the feedback network of the amplifier, and on the resulting transfer function. The consequent effects include a partial nulling of the input coil's self-inductance, as well as resonant peaking in the closed-loop response that depends on the impedance of the input coil circuit.

**Index Terms**—Feedback amplifiers, Particle detectors, SQUIDs, TES.

## I. INTRODUCTION

THE Superconducting Quantum Interference Device (SQUID) Series Array Amplifiers (SSAAs) employed by the Cryogenic Dark Matter Search (CDMS) in the phonon pulse amplification and readout chain take advantage of the SQUID design given in [1], which includes a superconducting electrically-isolated flux-focusing washer. The associated room-temperature electronics are of the direct-readout type with a single-pole integrator, the theory and behavior of which are described in [2] and [3]. For further information on the CDMS phonon detection system, see [4]-[8]. A change in apparent input inductance, and thus amplifier bandwidth, is seen in SQUID operation between closed- and open-loop configurations. This bandwidth change is measurable and repeatable. It can be understood in terms of an additional source of inductive-coupled feedback between the input and feedback coils in the array. We also observe resonant peaking in the amplifier closed-loop frequency response, which,

Manuscript received 3 August 2010. This work was supported in part by the National Science Foundation under Grants PHY-0503641, PHY-0705052, PHY-0801708, PHY-0504224, PHY-0705078 PHY-0802575.

B. A. Hines and M.E. Huber are with the University of Colorado Denver, Denver, CO 80204 USA (phone: 303-556-4775; fax: 303-556-6257; e-mail: bruce.hines@ucdenver.edu; martin.huber@ucdenver.edu).

K. M. Sundqvist and D. N. Seitz are with the University of California, Berkeley, CA 94720 USA. (e-mail: kylesun@Cosmology.Berkeley.edu; dseitz@berkeley.edu).

according to [2] and [3], can result from the time delay and accompanying phase lag of the feedback signal. There is also mention of the coupling in [2] and [9]. In this paper we treat this phenomenon with a new theoretical model that accurately predicts our experimental results.

## I. TRANSFORMER EQUATIONS

If we consider that there exists a direct transformer coupling between the feedback and input branches of the SQUID amplifier, then we find, in addition to the typically assumed input-SQUID and feedback-SQUID coupling, a parallel feedback channel. Through the mechanism illustrated in Fig. 1a, this additional feedback signal is induced directly back into the input coil via  $M_{if}$ , then back again into the SQUID summing node via the input-SQUID mutual inductance.

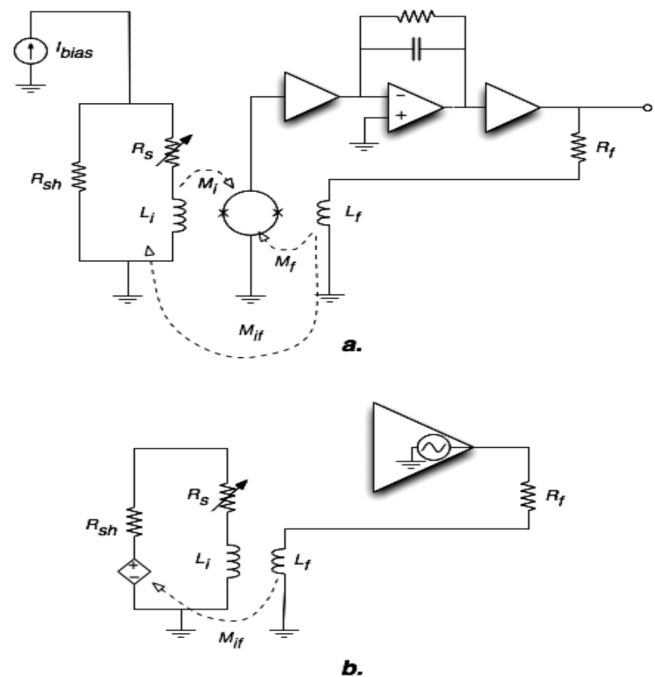


Fig 1. a) The CDMS flux-locked SSAA, depicted with the mutual inductance terms dominant in signal formation. We account for a mutual inductance ( $M_{if}$ ) directly between the feedback and input coils, which introduces an additional feedback factor. b) Driven by the amplifier output, the effect of the  $M_f$  contribution can be considered as a flux-induced voltage source in series with the input impedance, as per Lenz's law.

We use the following symbols:  $L_i$  is the input coil inductance,  $L_f$  is the feedback coil inductance  $M_{if}$  is the feedback-input mutual inductance (assumed symmetric),  $M_i$  is the input-SQUID mutual inductance,  $M_f$  is the feedback-SQUID mutual inductance,  $R_{sh}$  is the shunt resistance,  $R_s$  is the

sensor (Transition Edge Sensor or TES) variable resistance, and  $R_f$  is the feedback resistance. A dc current,  $I_{bias}$  sets the sensor at its optimum transition temperature and with  $R_{sh}$  ( $\ll R_s$ ) keeps a constant voltage across the sensor and input coil.

We can view this effect as a current-controlled voltage source in series with the input coil (the secondary transformer coil), as illustrated in Fig. 1b. The magnitude of the voltage is controlled by  $i_f$ , the feedback current, which in turn is determined by  $i_s$ , the total current through the input coil and sensor.

Transformer equations [10], derived from application of Kirchoff's voltage laws to both coil loops, give us a simple and yet general outcome: the current ratio in the two inductors. For the transformer circuit in Fig. 1, the current ratio is

$$\frac{i_{s\_ind}}{i_f} = \frac{-sM_{if}}{(R_{sh} + R_s + sL_i)}, \quad (1)$$

where  $i_{s\_ind}$  is the *induced* input current (a component of  $i_s$ ) and  $s$  represents complex frequency as in Laplace formalism.

Note that the frequencies of interest in the CDMS SQUID amplifier are *much* lower than the Josephson frequencies, so our analysis assumes that the coupling affects the input coil current due to induced emf but not the SQUID behavior [13].

Regardless of the polarity chosen for SQUID lock in our amplifier, when in stable operation the input coil current is always opposing the feedback current. Therefore, the minus sign of this term, due to Lenz's law, always *assists* the input coil current. This tells us that impedance is being lowered. It makes sense that the strength of this effect is proportional to the coupling  $M_{if}$ , and the denominator informs us that more impedance in the sensor line loop will logically diminish the *induced* sensor current. Also, as this effect induces more signal current, we can see that it opposes stability and may act as a positive feedback mechanism.

#### I. REVIEW OF CLOSED-LOOP SQUID AMPLIFIER OPERATION

We derived the transfer function of the closed-loop SQUID amplifier utilizing classic control theory and a "signals and systems" approach (e.g. [11]). The transfer function here relates ac sensor current to output voltage by the action of the amplifier. It takes the form [12]

$$H(s) = M_i \frac{\alpha(s)}{1 + \alpha(s)\beta(s)}, \quad (2)$$

where  $\alpha(s)$  is the open loop gain and  $\beta(s)$  is the feedback factor. The pre-factor of  $M_i$  is particular to our SQUID amplifier, and serves to convert the input current signal into proper units (of flux) at the SQUID summing node. The open loop gain,  $\alpha$ , is determined from the transducer (SQUID) chain at the input on up through the active electronics. So

$$\alpha(s) = \frac{1}{M_i} \frac{\partial V_{SQ}}{\partial i_s} A_{VG} \left( \frac{A_{int} \omega_{int}}{s + \omega_{int}} \right) = \frac{1}{M_i} \frac{G}{s + \omega_{int}}, \quad (3)$$

where  $\partial V_{SQ}/\partial i_s$  is the transresistance (or "responsivity") of the SQUID. This relates a change in current in the input coil to a change in SQUID voltage.  $A_{VG}$  is the voltage-to-voltage variable gain of the feedback chain, including preamp. The last term in parentheses represents the gain and frequency

dependence of the integrator, included in the circuit for dominant-pole compensation. The integrator has a gain of  $A_{int}$  and a cutoff-frequency of  $\omega_{int}$ . For ease of writing equations, we introduce the quantity  $G = G_0 \omega_{int}$ , the Gain-Bandwidth product (product of the dc gain and integrator frequency), which in our situation is a constant on the order of  $10^{10}$ .

We now consider, for purposes of comparison, an *ideal* SQUID amplifier, neglecting the coupling between the input and feedback coils. The standard feedback factor would be

$$\beta_0(s) = \frac{M_f}{R_f}. \quad (4)$$

This relates the amplifier output voltage back to the SQUID as a flux signal. We call this term  $\beta_0$ , rather than  $\beta$ , to distinguish it as the original *ideal* feedback term. It leads to the transfer function

$$H_{ideal}(s) = R_f \frac{M_i}{M_f} \left( \frac{1}{1 + R_f \frac{M_i}{M_f} \frac{(s + \omega_{int})}{G}} \right). \quad (5)$$

It is helpful to realize that the quantity,  $M_i/M_f$ , is equal to the ratio of the number of turns of the input coil to that of the feedback coil [4]. For the SSAAs used in CDMS,  $M_i/M_f = 10.5$ .

#### I. THE NEW FEEDBACK FACTOR

Looking at Fig. 2, we see a signal-flow diagram that puts our new situation into perspective.

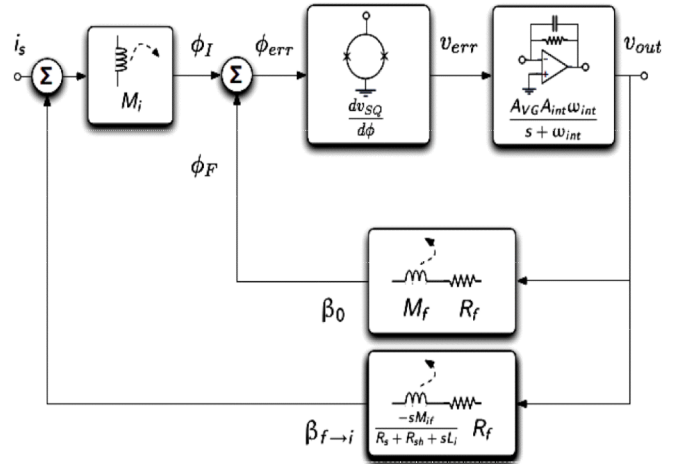


Fig. 2. A signal-flow diagram, including the additional feedback factor. Note that  $dV_{SQ}/d\phi$  was used to group the elements in a logical way, where  $\phi$  is the total flux through the SQUID loop.  $\phi_{err}$  and  $V_{err}$  represent the error signal from the summing node of the feedback system.  $V_{out}$  is the output voltage.

For the portion of sensor current determined by  $V_{out}$ , induced by the current through the feedback coil via the new feedback factor, we have

$$i_{s\_ind} = V_{out} \left[ \frac{1}{R_f} \left( \frac{-sM_{if}}{R_{sh} + R_s + sL_i} \right) \right]. \quad (6)$$

From here, this induces flux signal back into the SQUID as typical, by way of the factor  $M_i$ .

Re-expressed,

$$\beta_{f \rightarrow i}(s) = \frac{M_i}{R_f} \left( \frac{-sM_{if}}{R_{sh} + R_s + sL_i} \right). \quad (7)$$

It can be seen that our feedback factors, from the output amplifier voltage to the input branch current (or flux), are acting as conductances. They are also in parallel. Therefore, they add accordingly. The full feedback factor becomes

$$\beta(s) = \beta_0(s) + \beta_{f \rightarrow i}(s). \quad (8)$$

Making use of the relation

$$\frac{\partial V_{SQ}}{\partial i_s} = \frac{\partial V_{SQ}}{\partial \phi} \frac{\partial \phi}{\partial i_s} = \frac{\partial V_{SQ}}{\partial \phi} M_i, \quad (9)$$

we derive the improved transfer function

$$\begin{aligned} H(s) &= \frac{G}{s + \omega_{int} + \frac{G}{R_f} \left( \frac{M_f}{M_i} - \frac{sM_{if}}{R_{sh} + R_s + sL_i} \right)} \\ &= R_f \frac{M_i}{M_f} \left( \frac{1}{1 + R_f \frac{M_i}{M_f} \frac{(s + \omega_{int})}{G} - \frac{M_i}{M_f} \frac{sM_{if}}{R_{sh} + R_s + sL_i}} \right). \end{aligned} \quad (10)$$

Note that this transfer function differs from the ideal one by an additional frequency-dependent term in the denominator.

In practice, due to the frequency dependence of the input circuit, from its single-pole response as a series RL loop, the full transfer function becomes

$$\begin{aligned} H_{full}(s) &= R_f \frac{M_i}{M_f} \left( \frac{1}{1 + R_f \frac{M_i}{M_f} \frac{(s + \omega_{int})}{G} - \frac{M_i}{M_f} \frac{sM_{if}}{R_{sh} + R_s + sL_i}} \right) \\ &\cdot \left( \frac{1}{1 + s \frac{L_i}{R_{sh} + R_s}} \right). \end{aligned} \quad (11)$$

A pole from the input circuit ( $-(R_{sh} + R_s)/L_i$ ) cancels the zero from the feedback factor, so the denominator is second-order.

It is informative to take the case where the open-loop gain is assumed to be infinite. Then,

$$H(s) \approx \frac{M_i}{\beta(s)} = \left( \frac{\frac{M_i}{M_f} R_f}{1 - k \sqrt{\frac{L_f}{L_i}} \frac{M_i}{M_f}} \right) \frac{s - \left( \frac{-(R_s + R_{sh})}{L_i} \right)}{s - \left( \frac{-(R_s + R_{sh})}{L_i - \frac{M_i}{M_f} k \sqrt{L_i L_f}} \right)}, \quad (12)$$

where  $k$  is the inductive coupling coefficient between the input and feedback coils. The expression is put intentionally into zero-pole-gain form. The first term in parentheses is the gain term, and we can recognize the factor of  $(M_i/M_f)R_f$ , which is the dc gain in the ideal SQUID amp transfer function. Also, we have a zero at  $-(R_s + R_{sh})/L_i$  and a pole at  $-(R_s + R_{sh})/(L_i - (M_i/M_f)M_{if})$ . The input coil circuit itself has a natural pole at  $-(R_s + R_{sh})/L_i$ , which the amplifier nulls with a zero at precisely the same frequency. However, the amplifier with ideal (infinite) open-loop gain also imposes its pole at a higher frequency. In effect, this is actively raising the innate bandwidth of the input coil. Perhaps we could call this an active inductance lowering, where the effective input-coil inductance becomes

$$L_{eff} = L_i - \frac{M_i}{M_f} k \sqrt{L_i L_f} = L_i - \frac{M_i}{M_f} M_{if}. \quad (13)$$

## I. EXPERIMENTAL INVESTIGATION

To test this model, we made open-loop and closed-loop measurements using CDMS SSAAs to determine values for the various parameters in the full transfer function (11).

### A. Resistance in series with the input coil, $R_i$

For our tests, we shorted the shunt resistor, which is located on the SQUID chip, with the input coil. This forms a closed loop, not grounded, with  $R_{sh}$  plus any parasitic resistance from the shorting wires and  $L_i$ . We call the total series resistance  $R_i$ . In the equations above this is the same as  $R_{sh} + R_s$ . Note that for these measurements, the sensor (TES) was not in the input circuit.

Two separate measurement techniques resulted in the same value of  $R_i$ . In both of these the amplifier input was the thermal noise current from this input resistance. In closed loop, this current is amplified by a factor of  $R_f(M_i/M_f)$  at low frequencies (see transfer function in (11)). In open loop, the current is amplified by the value of the slope of the  $V$ - $\phi$  curve, as measured on an oscilloscope (i.e.  $\partial V_{SQ}/\partial i_s$ , a constant at the SQUID array's operating range [2]). The output in both cases is noise voltage that we measured with a spectrum analyzer and from which  $R_i$  was calculated. We used this value of  $R_i$  in the other tests.

### A. Self inductance of the input coil in open-loop, $L_i$

We determined the value of  $L_i$  by three different methods, all of which were in agreement.

1) A four-wire impedance measurement of the SSAA input coil, with two wire bonds to each of two pads on the SQUID chip, found  $L_i$  from the slope of the impedance vs. frequency curve. This entailed sweeping the frequency of a sinusoidal current of known amplitude through one pair of the four-wire setup and determining the amplitude of the voltage across the other pair with an oscilloscope. Parasitic inductance was measured separately and subtracted.

2) We determined the bandwidth of the SSAA operated in open loop by observing on a spectrum analyzer the -3 dB point of the frequency response with the noise current as the input. In this configuration, the pole of the input circuit dominates, resulting in a cutoff frequency of  $R_i / (2\pi L_i)$ .

3) A third approach found the same value of  $L_i$  as well as a value for  $M_{if}$ , the mutual inductance between the input and feedback coils. A curve fit to the results of this measurement supports our direct feedback model. This test involved use of a signal generator sourced via the feedback resistor to sweep a sinusoidal current through the feedback coil, and measuring the output voltage of the SSAA in open loop. We then see the changes in flux with frequency due to the *induced* current in the input coil. Using this setup, the only frequency dependent element is the full feedback factor,  $\beta(s)$ . From (8) we get

$$H_{source\_fdbk}(s) = const \cdot \left( 1 - \frac{M_i}{M_f} \frac{sM_{if}}{R_i + sL_i} \right). \quad (14)$$

This gives us a zero at  $-R_i/L_{eff}$  and a pole at  $-R_i/L_i$ . Fig. 3 shows good agreement between the measured output and a curve fit using (14). We performed our curve-fitting using R software [14].

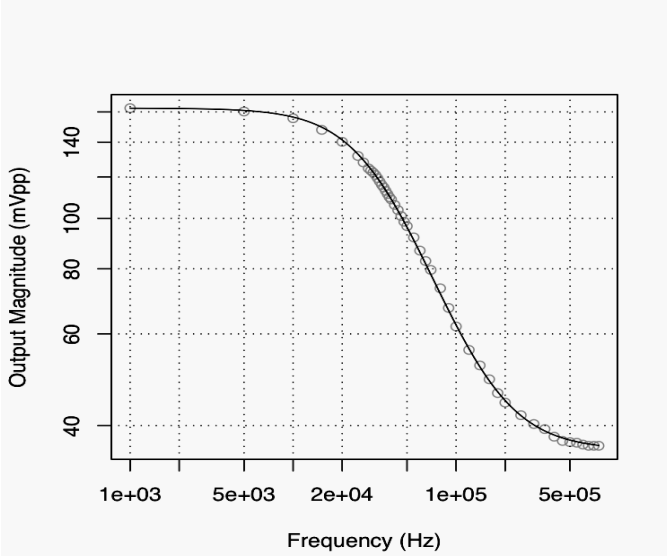


Fig. 3. Output of SQUID amplifier in open loop. A sinusoidal current was sent through the feedback coil of the SSAA. The small circles show the measured data. The black curve is the result of a curve fit done on the data points using the equation for the full feedback factor,  $\beta(s)$  (14).

#### A. Closed-loop measurement

With the noise current as the input, we measured the closed-loop noise voltage output of a CDMS SQUID amplifier with a spectrum analyzer. The data points are represented in Fig. 4 by the small, gray circles. A curve fit using (11) found parameter estimates of  $L_i = 460$  nH and  $M_{if} = 35$  nH.

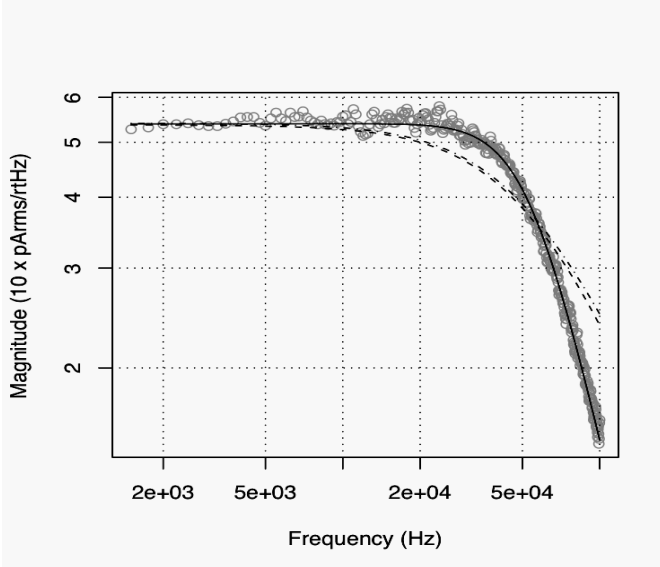


Fig. 4. Frequency response of SQUID amplifier in closed-loop operation. Circles represent data points. Black curve is the result of a curve fit using (11). Dash-dotted curve shows hypothetical frequency response of a single  $L/R$  pole from the input circuit, which implies that the *effective* value of  $L_i$  would be 72 nH. Dashed curve shows hypothetical response using the *ideal* transfer function (5) and the same *effective* value of  $L_i$ .

We used measured values of  $R_i = 0.0235 \Omega$  and  $R_f = 1230 \Omega$ , and a calculated value of  $G$  based on system components.

This value of  $L_i$  agrees with what was found by open-loop measurement (480 nH). The two types of curve fit shown in Fig. 3 and Fig. 4 both result in consistent values of  $M_{if}$ .

All three curves in Fig. 4 have about the same -3 dB frequency ( $\sim 53$  kHz), but our derived full transfer function

clearly matches the experimental values the best. In open loop, the bandwidth was 7.75 kHz (the frequency of the actual  $L_i/R_i$  pole from the input circuit). We see that bandwidth and *effective* input inductance differ by a factor of nearly seven between open-loop and closed-loop operation.

Using (13), the calculated value of  $L_{eff}$  is 84 nH. We get this same value using (11) when setting the open-loop gain to infinity. If we assume that  $L_f = L_i/10.5^2$ , based on the turns ratio of the input and feedback coils and on the effect of the flux-focusing washer, the coupling constant,  $k$ , is 0.82.

#### A. Fluctuations of input circuit impedance

In Fig. 5, we see the changes in SQUID amp output, based on (11), with  $R_i$  ranging over values similar to those of the current CDMS detectors when in operation. We see the resonant peaking increasing as  $R_i$  increases. At values above about  $1.3 \Omega$ , the peaking disappears again. In actuality, the quantity  $R_s$  is itself frequency dependent, and would more accurately be named  $Z_{TES}(s)$  in use of (11).

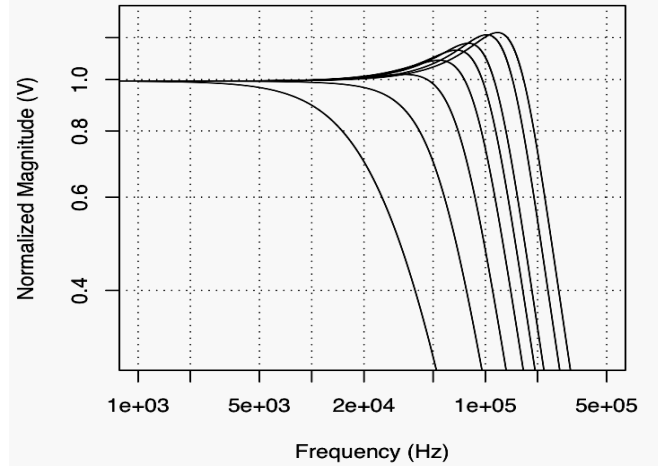


Fig. 5. Closed-loop frequency response with various values of the input resistance. From left to right,  $R_i = 0.01 \Omega, 0.0235 \Omega, 0.04 \Omega, 0.06 \Omega, 0.08 \Omega, 0.1 \Omega, 0.15 \Omega$ , and  $0.2 \Omega$ .

We can write (11) in the standard second-order form [15]:

$$H_{full}(s) = \frac{const}{\left(s^2 + s\frac{\omega_0}{Q} + \omega_0^2\right)}, \quad (15)$$

where  $\omega_0$  (the pole frequency) and  $Q$  (pole  $Q$  factor) are expressed in parameters of the SSAA and associated electronics, all of which are part of (11). The values of these parameters can be measured or calculated, and so we can obtain values for  $\omega_0$  and  $Q$ . If  $Q > 0.5$ , the poles are complex; and if  $Q = 0.707$ , the response is maximally flat. For the experiment shown in Fig. 4,  $Q \approx 0.65$  and  $\omega_0 \approx 3.2 \cdot 10^5$ . We see examples of changes in closed-loop frequency response due to different values of  $Q$  (which depends on  $R_i$ ) in Fig. 5.

This approach could be useful in design of similar SQUID amplifier systems.

## REFERENCES

- [1] M. E. Huber, et al., DC SQUID Series Array Amplifiers with 120 MHz bandwidth (Corrected), *IEEE Transactions on Applied Superconductivity*, Vol. 11, No. 2, pp. 4048-4053, 2001.
- [2] D. Drung, Advanced SQUID read-out electronics, *SQUID Sensors: Fundamentals, Fabrication and Applications*, Kluwer Academic Publishers, Netherlands, pp. 63-116, 1996.
- [3] D. Drung, High- $T_c$  and low- $T_c$  dc SQUID electronics, *Superconductor Science and Technology*, Vol. 16, pp. 1320-1336, 2003.
- [4] D. Akerib, et al., Design and performance of a modular low-radioactivity readout system for cryogenic detectors in the CDMS experiment, *Nuclear Instruments and Methods in Physics Research A*, Vol. 591, pp. 476-489, 2008.
- [5] K. Irwin, S. Nam, B. Cabrera, B. Chugg, G. Park, R. Welty, and J. Martinis, A self-biasing cryogenic particle detector utilizing electrothermal feedback and a SQUID readout, *IEEE Transactions on Applied Superconductivity*, Vol. 5, No. 2, pp. 2689-2693, 1995.
- [6] K. Irwin, G. Hilton, Transition-edge sensors, *Cryogenic Particle Detection*, C. Ends (Ed.), Springer Verlag, Berlin, 2005.
- [7] K. Irwin, An application of electrothermal feedback for high resolution cryogenic particle detection, *Applied Physics Letters*, Vol. 66, No. 15, pp. 1998-2000, 1995.
- [8] R. Welty, J. Martinis, A series array of dc SQUIDs, *IEEE Transactions on Magnetics*, Vol. 27, No. 2, pp. 2924-2926, 1991.
- [9] P.A.J. de Corte, J. Beyer, S. Deiker, G.C. Hilton, K.D. Irwin, M. MacIntosh, S.W. Nam, C.D. Reintsema, L.R. Vale, and M.E. Huber, Time-division superconducting quantum interference device multiplexer for transition-edge sensors, *Review of Scientific Instruments*, Vol. 74, No. 8, 2003, pp. 3807-3815.
- [10] A. Boyajian, Fundamental principles of polarity, phase rotation, and voltage diagrams of transformers, *General Electric Review*, Vol. XXIII, No. 5, General Electric Company, Schenectady, NY, May 1920.
- [11] A. V. Oppenheim, A. S. Willsky, S. H. Nawab, *Signals and Systems*, 2<sup>nd</sup> ed., Upper Saddle River, NJ: Prentice Hall, 1997, pp. 423 - 460.
- [12] A. V. Oppenheim, A. S. Willsky, S. H. Nawab, *Signals and Systems*, 2<sup>nd</sup> ed., Upper Saddle River, NJ: Prentice Hall, 1997, pp. 816 - 866.
- [13] C. D. Tesche, Analysis of strong inductive coupling on SQUID systems, *IEEE Trans Mag*, MAG-19, No. 3, pp. 458-460, 1983.
- [14] R.app GUI 1.23 (4932), S.Urbaneck & S.M.Iacus, © R Foundation for Statistical Computing, 2008.
- [15] A. Sedra, K. Smith, *Microelectronic Circuits*, 5<sup>th</sup> ed., Oxford University Press, New York, 2004, pp 836 - 845.